

## Minimum Weight Design of Rotorcraft Blades with Multiple Frequency and Stress Constraints

Aditi Chattopadhyay\*

Analytical Services and Materials, Inc.

Hampton, Virginia

and

Joanne L. Walsh†

NASA Langley Research Center

Hampton, Virginia

### Introduction

**A**N important consideration in helicopter rotor blade design is to reduce vibration without increasing blade weight. Rotor blade vibration can be reduced by separating its natural frequencies from the harmonics of the airloads or the excitation frequencies to avoid resonance. In the conventional design process this is usually done by post-design addition of nonstructural masses, which often leads to weight penalties. Today, one of the more promising design approaches is the application of optimization techniques during the design process to reduce vibration.<sup>1,5</sup> Some recent work is devoted to reducing vibration of modal shaping<sup>1</sup> or by controlling the vertical hub shears and moments.<sup>2</sup> An early attempt at optimum blade design for proper placement of natural frequencies is due to Peters,<sup>3</sup> who addresses the optimum design of a rectangular blade with frequency and autorotational inertia constraint. Frequency placement alone was also addressed in Ref. 4 using the optimality criteria approach. In the problem addressed in this Note, blade weight is the objective function and constraints are imposed on natural frequencies, autorotational inertia, and centrifugal stress. This is an extension of the work of Ref. 5, where only the frequencies of first flapping dominated and first lead-lag dominated blade modes were constrained, without any constraint on blade stress.

### Blade Model

The blade model includes a nonuniform box beam located inside the airfoil. Its total weight  $W$  has two components,  $W_b$  and  $W_o$ , where  $W_b$  denotes the box beam weight and  $W_o$  represents the nonstructural weight of the blade, including the weight of the skin, honeycomb, etc., along with the weight of the tuning masses added to the blade. The blade is discretized into finite segments and the blade weight in discretized form is given as

$$W = \sum_{j=1}^N \rho_j A_j L_j + \sum_{j=1}^N W_{oj} \quad (1)$$

where  $N$  denotes the total number of segments and  $\rho_j$ ,  $A_j$ ,  $L_j$ , and  $W_{oj}$  denote the density, the cross sectional area, the length, and the nonstructural weight of the  $j$ th segment, respectively. The autorotational inertia ( $AI$ ) of the blade is calculated as

$$AI = \sum_{j=1}^N W_j r_j^2 \quad (2)$$

Presented as Paper 88-2337 at the AIAA/ASME/ASCE/AHS/ASC Structures, Structural Dynamics, and Materials Conference, Williamsburg, VA, April 18–20, 1988; received May 21, 1988; revision received March 28, 1989. Copyright © 1989 American Institute of Aeronautics and Astronautics, Inc. No copyright is asserted in the United States under Title 17, U.S. Code. The U.S. Government has a royalty-free license to exercise all rights under the copyright claimed herein for Governmental purposes. All rights are reserved by the copyright owner.

\*Research Scientist. Member AIAA.

†Research Engineer. Member AIAA.

0982-CP, 1984.

<sup>2</sup>Nixon, M. W., 1987, "Extension-Twist Coupling of Composite Circular Tubes and Application to Tilt Rotor Blade Design," *Proceedings of the 28th Structures, Structural Dynamics and Materials Conference*, AIAA Paper No. 87-0772, 1987, pp. 295–303.

<sup>3</sup>Bauchau, O. A., Coffenberry, B. S., and Rehfield, L. W., "Composite Box Beam Analysis: Theory and Experiments," *Journal of Reinforced Plastics and Composites*, Vol. 6, 1987, pp. 25–35.

<sup>4</sup>Simon, L., "A Set of Finite Elements Developed for the Dynamic Computation of Composite Helicopter Blades," ONERA TP 1981-87, 1981.

<sup>5</sup>Simo, J.C. and Vu-Quoc, L., "On the Dynamics of Flexible Beams Under Large Overall Motions – The Plane Case: Part I," *Journal of Applied Mechanics*, Vol. 53, No. 4, 1986, pp. 849–854.

<sup>6</sup>Danielson, D. A. and Hodges, D. H., "Nonlinear Beam Kinematics by Decomposition of the Rotation Tensor," *Journal of Applied Mechanics*, Vol. 54, No. 2, 1987, pp. 258–262.

<sup>7</sup>Hodges, D. H., "Nonlinear Beam Kinematics for Small Strains and Finite Rotations," *Vertica*, Vol. 11, No. 3, 1987, pp. 573–589.

<sup>8</sup>Danielson, D. A. and Hodges, D. H., "A Beam Theory for Large Global Rotation, Moderate Local Rotation, and Small Strain," *Journal of Applied Mechanics*, Vol. 55, No. 1, 1988, pp. 179–184.

<sup>9</sup>Parker, D. F., "An Asymptotic Analysis of Large Deflections and Rotations of Elastic Rods," *International Journal of Solids and Structures*, Vol. 15, 1979, pp. 361–377.

<sup>10</sup>Hong, C.-H. and Chopra, I., "Aeroelastic Stability of a Composite Blade," *Journal of the American Helicopter Society*, Vol. 30, No. 2, 1985, pp. 57–67.

<sup>11</sup>Hong, C.-H., and Chopra, I., "Aeroelastic Stability Analysis of a Composite Bearingless Rotor Blade," *Journal of the American Helicopter Society*, Vol. 31, No. 4, 1986, pp. 29–35.

<sup>12</sup>Hegemier, G. A. and Nair, S., "A Nonlinear Dynamical Theory for Heterogeneous, Anisotropic, Elastic Rods," *AIAA Journal*, Vol. 15, No. 1, 1977, pp. 8–15.

<sup>13</sup>Mansfield, E. H. and Sobey, A. J., "The Fiber Composite Helicopter Blade-Part 1: Stiffness Properties-Part 2: Prospects for Aeroelastic Tailoring," *Aeronautical Quarterly*, Vol. 30, 1979, pp. 413–449.

<sup>14</sup>Mansfield, E. H., "The Stiffness of a Two-Cell Anisotropic Tube," *Aeronautical Quarterly*, Vol. 32, 1981, pp. 338–353.

<sup>15</sup>Rehfield, L. W., "Design Analysis Methodology for Composite Rotor Blades," June 1985, AFWAL-TR-85-3094, pp. (V(a)-1)–(V(a)-15).

<sup>16</sup>Hodges, R. V., Nixon, M. W., and Rehfield, L. W., "Comparison of Composite Rotor Blade Models: A Coupled-Beam Analysis and an MSC/NASTRAN Finite-Element Model," NASA TM 89024, 1987.

<sup>17</sup>Rehfield, L. W. and Murthy, P. L. N., "Toward a New Engineering Theory of Bending: Fundamentals," *AIAA Journal*, Vol. 20, No. 5, 1982, pp. 693–699.

<sup>18</sup>Wörndle, R., "Calculation of the Cross Section Properties and the Shear Stresses of Composite Rotor Blades," *Vertica*, 1982, Vol. 6, pp. 111–129.

<sup>19</sup>Bauchau, O. A., "A Beam Theory for Anisotropic Materials," *Journal of Applied Mechanics*, Vol. 52, 1985, pp. 416–422.

<sup>20</sup>Bauchau, O. A. and Hong, C. H., "Large Displacement Analysis of Naturally Curved and Twisted Composite Beams," Rensselaer Polytechnic Institute, Troy, NY, 1986, RTC Report D-86-1.

<sup>21</sup>Bauchau, O. A., and Hong, C. H., "Finite Element Approach to Rotor Blade Modeling," *Journal of the American Helicopter Society*, Vol. 32, No. 1, 1987, pp. 60–67.

<sup>22</sup>Kosmatka, J. B., "Structural Dynamic Modeling of Advanced Composite Propellers by the Finite Element Method," Ph.D. Dissertation, University of California, Los Angeles, 1986.

<sup>23</sup>Giavotto, V., Borri, M., Mantegazza, P., Ghiringhelli, G., Carmaschi, V., Maffioli, G. C., and Mussi, F., "Anisotropic Beam Theory and Applications," *Computers and Structures*, Vol. 16, 1983, pp. 403–413.

<sup>24</sup>Borri, M. and Mantegazza, P., "Some Contributions on Structural and Dynamic Modeling of Rotor Blades," *L'Aerotecnica Missili e Spazio*, Vol. 64, No. 9, 1985, pp. 143–154.

<sup>25</sup>Borri, M. and Merlini, T., "A Large Displacement Formulation for Anisotropic Beam Analysis," *Meccanica*, Vol. 21, 1986, pp. 30–37.

<sup>26</sup>Lee, S. W., and Stemple, A. D., "A Finite Element Model for Composite Beams with Arbitrary Cross-Sectional Warping," *AIAA Journal*, Vol. 26, No. 12, 1988, pp. 1512–1520.

<sup>27</sup>Stemple, A. D., and Lee, S. W., "A Finite Element Modeling for Composite Beams Undergoing Large Deflections with Arbitrary Cross Sectional Warping," *International Journal of Numerical Methods in Engineering*, Vol. 28, No. 9, 1989, pp. 2143–2163.

where  $W_j$  is the total weight and  $r_j$  is the distance from the root to the center of the  $j$ th segment. The expression for the blade stress is

$$\alpha_i = \sum_{j=1}^N M_j \Omega^2 r_j / A_i \quad (3)$$

where  $\sigma_i$  is the stress due to centrifugal forces,  $A_i$  the cross-sectional area of the  $i$ th segment,  $M_j$  the total mass of the  $j$ th segment, and  $\Omega$  the blade rpm.

### Optimization Formulation

The optimization problem is posed as follows:

$$\text{minimize } W(\phi)$$

where weight  $W$  is given by Eq. (1) and  $\phi$  denotes the vector of design variables, subject to the normalized constraints

$$g_k(\phi) = (f_k/f_{k_U}) - 1 \leq 0 \quad k = 1, 2, \dots, 5 \quad (4)$$

$$g_{k+5}(\phi) = 1 - (f_k/f_{k_L}) \leq 0 \quad k = 1, 2, \dots, 5 \quad (5)$$

$$g_{11}(\phi) 1 - (AI/\alpha) \leq 0 \quad (6)$$

$$g_{11+k}(\phi) = 1 - \sigma_{\max}/(\sigma_k FS) \leq 0 \quad k = 1, 2, \dots, N \quad (7)$$

and side constraints

$$\phi_{i_L} \leq \phi_i \leq \phi_{i_U} \quad (8)$$

In Eqs. (4) and (5), the frequencies associated with the first five elastic modes of coupled vibration are denoted by  $f_1, f_2, f_3, f_4$ , and  $f_5$  (includes three lead-lag and two flapping) and  $f_{k_U}, f_{k_L}$  denote the upper and lower bounds on the  $k$ th frequency  $f_k$ . In Eq. (6),  $\alpha$  represents the minimum prescribed autorotational inertia value. In Eq. (7),  $\sigma_k$  is the stress in the  $k$ th segment given by Eq. (3),  $\sigma_{\max}$  the maximum allowable stress in the blade and  $FS$  a factor of safety. In Eq. (8),  $\phi_i$  denotes the  $i$ th design variable and  $\phi_{i_U}$  and  $\phi_{i_L}$  represent the associated upper and lower bounds, respectively. The design variable include box beam dimensions, taper ratio, and magnitudes of the nonstructural weights located inside the box beam.

The modal analysis portion of the program CAMRAD,<sup>6</sup> which uses a modified Galerkin approach, is used for calculating the frequencies. The general-purpose optimization program CONMIN<sup>7</sup> and a linear approximation technique that

uses Taylor series expansion is used for optimization. A sensitivity analysis part of the procedure, and analytical expressions obtained for the derivatives of the objective function, the autorotational inertia constraint, and the stress constraints. A central-difference scheme is used for the derivative of the frequency constraints.

### Test Problem

The reference blade (Fig. 1) is articulated and has a rigid hub. It has a rectangular planform, a pretwist, and a root spring that allows torsional motion. A box beam with unequal vertical wall thickness is located inside the airfoil. It is assumed that the box beam contributes to the blade stiffness, and that the contributions of the skin, honeycomb, etc., to the blade stiffness are neglected. The details for calculating the box beam section properties can be found in Ref. 5. The properties of the box beam located inside the airfoil (Fig. 1) are:  $h = 0.117$  ft,  $b = 0.463$  ft,  $\rho = 8.645$  slug/ft<sup>3</sup>,  $E = 2.340 \times 10^9$  lb/ft<sup>2</sup>,  $\sigma_{\max} = 1.93 \times 10^7$  lb/ft<sup>2</sup>, and  $FS = 3$ . The blade is discretized into 10 segments and details of the blade segment data are presented in Refs. 3 and 8. The frequencies of interest of the reference blade are presented in Table 1. The first three lead-lag and the first two flapping dominated modes are away from the critical frequencies and need not be improved further. Therefore, the frequency windows for the optimum blade are set to be within  $\pm 1\%$  of these values.

### Results and Discussion

Some typical results obtained by applying the optimization procedure to the design of both rectangular and tapered rotor blades are presented in Table 1 and Figs. 1–3. Further results, can be found in Ref. 8. In the case of the rectangular blade, the taper ratio  $\lambda$  is held constant, i.e.,  $\lambda = 1.0$ . In all cases, convergence is typically achieved in 8–10 cycles (full analysis). A convergence tolerance of  $0.5 \times 10^{-5}$  is used for three consecutive values of the objective function in this study. Table 1, column 1 represents the reference blade data. Columns 2 and 3 give the corresponding information for the optimum design with constraints on five frequencies, autorotational inertia, and centrifugal stress for the rectangular and tapered blades, respectively. The table indicates that the optimum rectangular blade is 2.67 and 4.74% lighter than the reference blade, and the optimum tapered blade is 6.21% lighter than the reference blade. The first lead-lag frequency ( $f_1$ ) is at its prescribed upper bound after optimization and the autorotational inertia constraint is active in all cases. Some typical design variable distributions are presented in Figs. 1–3. Fig. 1 presents the optimum and the reference blade box beam horizontal wall thickness ( $t_1$ ) distributions along the blade span for the rectangular and tapered blades. In both cases, the optimum blade has a larger value of  $t_1$  than the reference blade at the blade tip and in case of the tapered blade the value of  $t_1$  at the blade root for the optimum blade is much smaller than the reference blade value. The larger design variable values toward the blade tip are

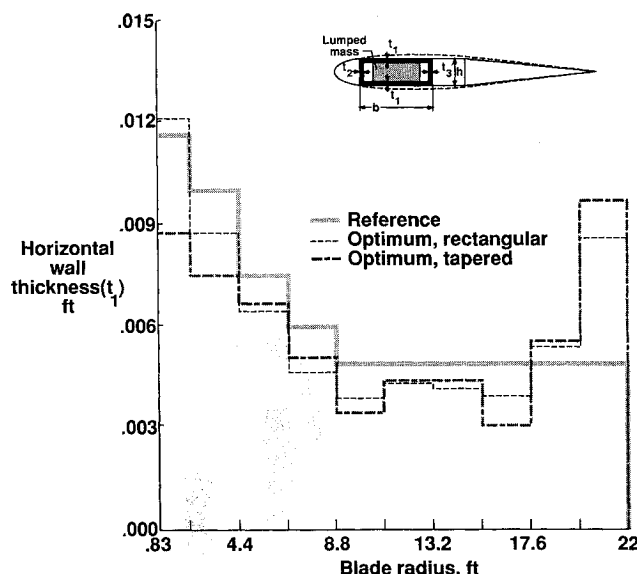


Fig. 1 Box beam horizontal wall thickness ( $t_1$ ) distribution; reference, optimum.

Table 1 Optimization results

	Frequency bounds		Reference	Optimum	
	Upper	Lower		Rectangular	Tapered
$f_1$ (Hz)	12.162	12.408	12.285	12.408	12.408
$f_2$ (Hz)	15.936	16.258	16.098	16.075	16.066
$f_3$ (Hz)	20.704	21.122	20.913	21.081	20.888
$f_4$ (Hz)	34.272	34.966	34.62	34.823	34.678
$f_5$ (Hz)	35.502	36.219	35.861	35.507	35.507
$\lambda_h$			1.0	1.0	1.490
Autorotational inertia (lb-ft <sup>2</sup> )			571.3	571.3	517.3
Blade weight (lb)			98.27	93.613	92.16
Percent reduction in blade weight <sup>a</sup>			—	4.74	6.212

<sup>a</sup>From reference blade.

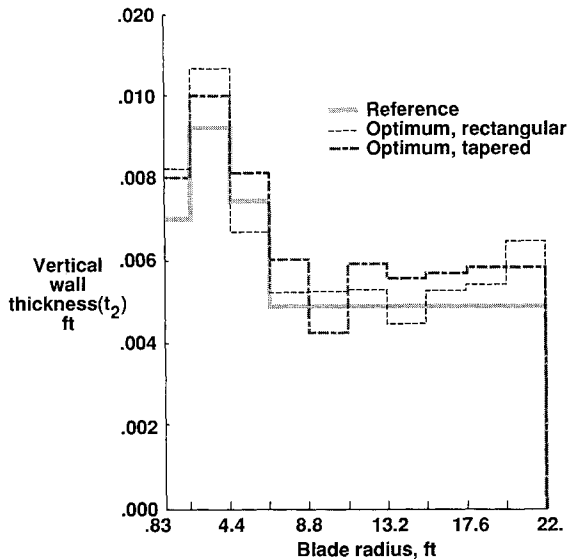


Fig. 2 Box beam vertical wall thickness ( $t_2$ ) distributions; reference, optimum.

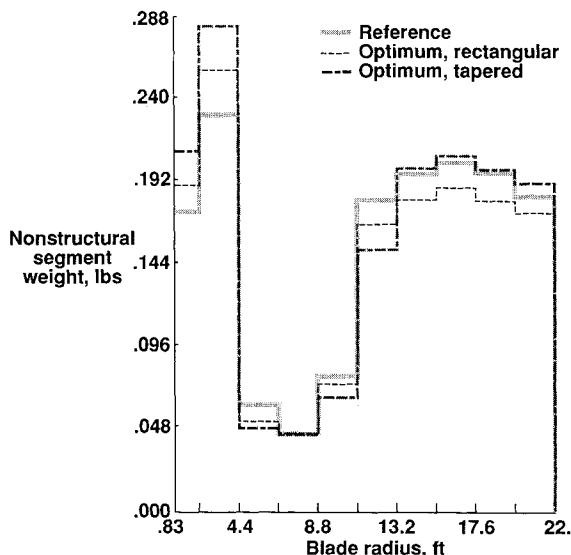


Fig. 3 Nonstructural segment weight distributions; reference, optimum.

caused by the presence of the autorotational inertia constraint which encourages the addition of mass at locations outboard. Figure 2 presents the box beam vertical wall thickness ( $t_2$ ) distributions for the reference and the optimum blades. Once again, the autorotational inertia constraint plays a big role in increasing the value of  $t_2$  at blade tip for the rectangular and the reference blades. However, the increase is not as significant as in the case of  $t_1$ . The nature of these thickness distributions are also different, as  $t_1$  primarily affects the flapping frequency and  $t_2$  the lead-lag frequency. Figure 3 depicts the optimum

and the reference blade nonstructural segment weight distributions along the blade radius for the rectangular and tapered blades. For the rectangular blade the optimum blade has lower nonstructural weight throughout the blade span. However, for the tapered blade the optimum blade has larger nonstructural weight towards the tip than the reference blade. This is because the blade is being tapered and has reduced structural weight at the blade tip. Therefore, in order to satisfy the autorotational inertia constraint, the nonstructural weight at the tip must increase. Even so, the total weights of the optimum blade are still lower than the reference blade.

A comparison of the results of the study with those obtained in Ref. 5 shows that, with an increase in the number of constraints, the optimum blade weight increases along with significant changes in the design variable distributions for both the rectangular and the tapered blades.

### Concluding Remarks

A procedure is described for the minimum weight design of helicopter rotor blades with constraints on multiple coupled flag-lag natural frequencies, autorotational inertia, and centrifugal stress. Optimum designs of blades with both rectangular and tapered planforms are obtained in typically 8–10 cycles.

The results of the study indicate that a significant reduction in blade weight is possible, even with constraints on multiple natural frequencies, for both the rectangular and the tapered blades. The optimization process tends to redistribute mass towards the blade tip due to the presence of the autorotational inertia constraint. The inclusion of multiple frequency constraints affects the optimum blade weight as well as the design variable distributions.

### References

- <sup>1</sup>Taylor, R. B., "Helicopter Vibration Reduction by Rotor Blade Modal Shaping," *Proceedings of the 38th Annual Forum of the AHS*, May 1982.
- <sup>2</sup>Friedmann, P. P. and Shantakumaran, P., "Optimum Design of Rotor Blades for Vibration Reduction in Forward Flight," *Proceedings of the 39th Annual Forum of the AHS*, May 1983.
- <sup>3</sup>Peters, D. A., Ko, T., and Rossow, M. P., "Design of Helicopter Rotor Blades for Desired Placement of Natural Frequencies," *Proceedings of the 39th Forum of the AHS*, May 1983.
- <sup>4</sup>Hanagud, S., Chattopadhyay, A., Yillikci, Y. K., Schrage, D., and Reichert, G., "Optimum Design of a Helicopter Rotor Blade," *Proceedings of the 12th European Rotorcraft Forum*, Paper No. 12, Sept. 1986.
- <sup>5</sup>Chattopadhyay, A. and Walsh, J. L., "Minimum Weight Design of Rectangular and Tapered Helicopter Rotor Blades With Frequency Constraints," *Proceedings of the 2nd International Conference of Rotorcraft Basic Research*, Feb. 1988. Also NASA TM 100561, Feb. 1988.
- <sup>6</sup>Johnson, W., "A Comprehensive Analytical Model of Rotorcraft Aerodynamics and Dynamics," Part I: Analysis Development, NASA TM 81182, June 1980.
- <sup>7</sup>Vanderplaats, G. N., "CONMIN—A Fortran Program for Constrained Function Minimization," *User's Manual*, NASA TM-62282, Aug. 1973.
- <sup>8</sup>Chattopadhyay, A. and Walsh, J. L., "Minimum Weight Design of Rotorcraft Blades With Multiple Frequency and Stress Constraints," *Proceedings of the AIAA/ASME/ASCE/AHS 29th Structures, Structural Dynamics and Materials Conference*, AIAA, Washington, D.C., April 1988. NASA TM-100569, March 1988.